Nuclear Physics B292 (1987) 330–348
North-Holland, Amsterdam

HIGH STATISTICS COMPUTATION OF THE TOPOLOGICAL SUSCEPTIBILITY OF SU(2) GAUGE THEORY

A.S. KRONFELD

Deutsches Elektronen-Synchrotron DESY, Hamburg, FR Germany

M.L. LAURSEN

NORDITA, København, Denmark

G. SCHIERHOLZ

Institut für Theoretische Physik, Universität Kiel and Deutsches Elektronen-Synchrotron DESY, Hamburg, FR Germany

U.-J. WIESE

Institut für Theoretische Physik, Universität Hannover, FR Germany

Received 21 August 1986
(Final review received 22 March 1987)

We use a recently proposed definition of the second Chern number of a lattice gauge field to compute the topological susceptibility of SU(2) gauge theory using numerical simulations. We describe the algorithm, which is very fast, so we are able to attain high statistics. For the computation of the susceptibility we have used 6^4, 8^4, and 10^4 lattices at values of the gauge coupling β ranging from 2.3 to 2.6. We address the issue of scaling and compare our results to those of other groups.

1. Introduction

This paper continues efforts [1–3] to investigate the topological structure of nonabelian gauge theories using the lattice formulation and numerical simulations. Our emphasis is on high statistics on large lattices. We used the combinatoric algorithm of Phillips and Stone [4], which proved to be the fastest. Here we discuss the topological susceptibility, which is the simplest quantity describing the influence of the topological properties of gauge theories. We also compare our results to those obtained previously. In a forthcoming publication [5] we discuss the implications of our calculations to the θ vacuum and the CP problem.

0550-3213/87/$03.50

The observable consequences of gauge field configurations with nontrivial topology enter through the anomalous divergence of the flavor singlet axial-vector current:

$$\tfrac{1}{2}\partial \cdot J^5 = -\frac{1}{16\pi^2}\mathrm{tr}\{F_{\mu\nu}{}^*F_{\mu\nu}\}, \qquad {}^*F_{\mu\nu} = \tfrac{1}{2}\varepsilon_{\mu\nu\rho\sigma}F_{\rho\sigma}. \tag{1.1}$$

Integrating eq. (1.1) over the space-time manifold M gives the topological charge,

$$Q = -\frac{1}{16\pi^2}\int_{\mathrm{M}} \mathrm{d}^4x\, \mathrm{tr}\{F_{\mu\nu}(x){}^*F_{\mu\nu}(x)\}, \tag{1.2}$$

which is a topological invariant and, neglecting boundary contributions (see refs. [6, 7]), assumes integer values. The anomaly (1.1) breaks the classical $\mathrm{U_A}(1)$ invariance of the QCD lagrangian, so that Goldstone's theorem is evaded: there need not be a nearly massless meson with the quantum numbers of the η'. Indeed, the mass of the η' is related to the topological susceptibility

$$\chi_t = \langle Q^2\rangle / V \tag{1.3}$$

(where V is the volume of the manifold) by [8]:

$$m_{\eta'}^2 + m_\eta^2 - 2m_{\mathrm{K}}^2 = 2N_f\chi_t/f_\pi^2, \tag{1.4}$$

as the number of colors $N_c \to \infty$. Owing to the qualitative successes of large N_c predictions, we therefore anticipate (using $N_f = 3$) that

$$\chi_t \approx (180\ \mathrm{MeV})^4, \tag{1.5}$$

even though the real world has only $N_c = 3$ and the simulations in this and previous papers have $N_c = 2$.

So far lattice calculations have been done on small lattices, at small values of β, and with low statistics. To extend the calculations to larger lattices and further into the continuum one needs an efficient algorithm for computing the topological charge of a lattice gauge field. Such an algorithm exists now, and this paper presents the first calculations of χ_t on lattices up to 10^4 *and* with high statistics. In sect. 2 we review the basic elements of topology, emphasizing the points important to lattice calculations. Sect. 3 covers the algorithm of ref. [4]. That algorithm is for simplicial lattices, so sect. 4 describes the interpolation from a hypercubical to a simplicial lattice, and adds some remarks about our computer program. In sect. 5 we present the results of our numerical simulations; in particular we compare and contrast our results for the susceptibility with those of other groups. We also suggest the topological susceptibility as a probe of scaling. In sect. 6 we argue that our

calculations of the topological susceptibility obey a certain bundle universality. Finally, sect. 7 contains some concluding remarks.

2. Topological charge

On the lattice the topological significance of eq. (1.2) is lost. Naive transcriptions of the integrand are not a total divergence, and ad hoc subtractions are needed to calculate χ_t [9]. Geometrically Q is a property of the principal bundle underlying the gauge field, and therefore one must concentrate on the topology of the principal bundle.

To do so, one covers the base manifold (i.e. space-time), chosen here to be a torus, by a set of cells:

$$\mathrm{M} = \mathrm{T}^4 = \bigcup_i \mathrm{c}_i \,, \tag{2.1}$$

with overlaps $\mathrm{c}_{ij} = \mathrm{c}_i \cap \mathrm{c}_j$ such that

$$\mathrm{c}_{ij} = \partial \mathrm{c}_i \cap \partial \mathrm{c}_j \,. \tag{2.2}$$

Since the lattice introduces a cellular structure anyway, it is quite natural to start from this perspective. In each cell c_i one can gauge transform by

$$A_\mu^{(i)}(x) = g_i^{-1}(x)\big[\partial_\mu + A_\mu(x)\big] g_i(x) \,, \tag{2.3}$$

so that the potential $A_\mu^{(i)}$ is everywhere nonsingular, but in different gauges in different cells. On c_{ij} the potentials are related by

$$A_\mu^{(i)}(x) = v_{ij}(x)\big[\partial_\mu + A_\mu^{(j)}(x)\big] v_{ji}(x) \,, \tag{2.4}$$

where

$$v_{ij}(x) = g_i^{-1}(x) g_j(x) = v_{ji}^{-1}(x) \,, \qquad x \in \mathrm{c}_{ij} \,. \tag{2.5}$$

The transition functions v_{ij} or, equivalently, the local sections g_i now carry all the information about the topology of the gauge field and completely determine the bundle.

Eq. (1.2) may now be rewritten:

$$Q = \sum_i \int_{\mathrm{c}_i} \mathrm{d}^4 x \, P \,, \qquad P = -\frac{1}{16\pi^2} \mathrm{tr}\big\{ F_{\mu\nu}^{(i)} * F_{\mu\nu}^{(i)} \big\} \,. \tag{2.6}$$

Since the Chern-Pontryagin density P is a total divergence,

$$P = \partial_\mu \Omega_\mu^{(0)}(i) \,, \tag{2.7}$$

one obtains

$$Q = \sum_i \int_{\partial c_i} d^3x_\mu \Omega_\mu^{(0)}(i) = \frac{1}{2!} \sum_{i,j} \int_{c_{ij}} d^3x_\mu \Delta\Omega_\mu^{(0)}(i,j), \tag{2.8}$$

where

$$\Delta\Omega_\mu^{(0)}(i,j) = \Omega_\mu^{(0)}(i) - \Omega_\mu^{(0)}(j), \tag{2.9}$$

$$\Omega_\mu^{(0)}(i) = -\frac{1}{8\pi^2}\varepsilon_{\mu\nu\rho\sigma}\mathrm{tr}\left\{ A_\nu^{(i)}\left[\partial_\rho A_\sigma^{(i)} + \tfrac{2}{3}A_\rho^{(i)}A_\sigma^{(i)}\right]\right\}. \tag{2.10}$$

Using relation (2.4) it is elementary to show that eq. (2.8) reduces to the expression (writing $c_{ijk} = c_i \cap c_j \cap c_k$)

$$Q = -\frac{1}{8\pi^2}\sum_{i<j<k}\int_{c_{ijk}} d^2x_{\mu\nu}\,\varepsilon_{\mu\nu\rho\sigma}\mathrm{tr}\left\{ (v_{ji}\partial_\rho v_{ij})(v_{jk}\partial_\sigma v_{kj})\right\}$$

$$+\frac{1}{24\pi^2}\sum_{i<j}\int_{c_{ij}} d^3x_\mu\,\varepsilon_{\mu\nu\rho\sigma}\mathrm{tr}\left\{ (v_{ij}\partial_\nu v_{ji})(v_{ij}\partial_\rho v_{ji})(v_{ij}\partial_\sigma v_{ji})\right\}, \tag{2.11}$$

which involves only the transition functions. This expression was first derived by Lüscher [10].

Ref. [11] shows that in SU(2) one can use the cochain reduction [12] to integrate (2.11) completely:

$$Q = Q^{(1)} + Q^{(2)} + Q^{(3)} + Q_\Sigma^{(3)}. \tag{2.12}$$

Each term in this expression for the charge is a sum of integer winding numbers,

$$Q^{(i)} = \sum n^{(i)}, \qquad Q_\Sigma^{(3)} = \sum n, \tag{2.13}$$

where n is associated with "lattice points," $c_i \cap c_j \cap c_k \cap c_l \cap c_m$, and $n^{(1)}$, $n^{(2)}$, and $n^{(3)}$ arise from gauge singularities along faces, plaquettes, and edges of the cell, respectively.

An alternative to the cochain reduction [11,12] is to write the charge in terms of the section g_i. From (2.5) and (2.11) one derives

$$Q = \frac{1}{24\pi^2}\sum_i \int_{\partial c_i} d^3x_\mu\,\varepsilon_{\mu\nu\rho\sigma}\mathrm{tr}\left\{ (g_i^{-1}\partial_\nu g_i)(g_i^{-1}\partial_\rho g_i)(g_i^{-1}\partial_\sigma g_i)\right\}, \tag{2.14}$$

which is the sum of winding numbers of the maps g_i on the boundaries of the c_i. It is also possible to integrate this expression because again the integrand is almost

everywhere a total divergence. Writing

$$g_i = \exp(i\alpha \cdot \tau) = \cos\alpha + i e_\alpha \cdot \tau \sin\alpha, \tag{2.15}$$

in SU(2) enables one to express the integrated of (2.14) as [11,12]

$$\frac{1}{24\pi^2}\varepsilon_{\mu\nu\rho\sigma}\mathrm{tr}\{(g_i^{-1}\partial_\nu g_i)(g_i^{-1}\partial_\rho g_i)(g_i^{-1}\partial_\sigma g_i)\} = \partial_\nu \omega_{\mu\nu}(i),$$

$$\omega_{\mu\nu}(i) = \frac{1}{8\pi^2}(\alpha - \sin\alpha\cos\alpha)\varepsilon_{\mu\nu\rho\sigma} e_\alpha \cdot (\partial_\rho e_\alpha \times \partial_\sigma e_\alpha), \tag{2.16}$$

except at singular points, $x_s \in \partial c_i$, at which $g_i = -1$, i.e. $\alpha = \pi$, where $\omega_{\mu\nu}(i)$ has a "vortex"

$$\frac{1}{8\pi}\varepsilon_{\mu\nu\rho\sigma} e_\alpha \cdot (\partial_\rho e_\alpha \times \partial_\sigma e_\alpha). \tag{2.17}$$

Applying Gauss' theorem and since $\partial(\partial c_i) = \varnothing$, eq. (2.14) reduces to [11]

$$Q = Q^{(1)} = \sum n^{(1)}(x_s; i), \tag{2.18}$$

with

$$n^{(1)}(x_s; i) = \frac{1}{8\pi}\int_{S_\varepsilon^2(x_s)} d^2x_{\mu\nu}\, \varepsilon_{\mu\nu\rho\sigma} e_\alpha \cdot (\partial_\rho e_\alpha \times \partial_\sigma e_\alpha) \in \mathbb{Z}, \tag{2.19}$$

where $S_\varepsilon^2(x_s)$ is a sphere of radius ε around the location x_s of a vortex, with orientation induced from ∂c_i.

Computationally, eqs. (2.13) and (2.18) also show special promise since they yield integers for each cell. Eq. (2.11), on the other hand, yields an integer only after summing over all cells. If one adopts the cellular structure of the lattice, eq. (2.18) has an advantage over eq. (2.13), at least at present values of the gauge coupling. Eq. (2.18) only requires locating singularities (of the section) leading to $Q^{(1)}$. Since

$$\sum n^{(1)}(x_s; i) \tag{2.20}$$

is also the winding number of g_i on ∂c_i, this is equivalent to determining how many times an arbitrary element of SU(2) – we call it the probe – falls into the image of ∂c_i under the map g_i.

Obviously, any definition of a smooth bundle to a lattice gauge field requires interpolation from the links to points missed by the discrete mesh of the lattice. An efficient procedure will oblige the computer to do as little explicit interpolation as possible. We started [13] to compute Q using eq. (2.18) and the section [14] for

Lüscher's interpolation [10]. This method involved "gauge cooling" (i.e. transforming to lattice Landau gauge) and subdividing the lattice until one could use geometrical methods to locate the singularities. This algorithm did not turn out to be optimal for SU(2) (see the end of sect. 4 for a comparison of algorithms), because the subdivision was costly. What one really wants is to extend the lattice gauge field to the bundle using only spherical polyhedra; then the search for singularities reduces to the computation of 4×4 determinants. Such an interpolation exists now [4], as we describe in the next section.

3. The algorithm

As the cells discussed above Phillips and Stone [4] consider the dual cells c_i surrounding sites x_i of a simplicial lattice, and their intersection with simplices σ, $c_i^\sigma = \sigma \cap c_i$. The simple dual geometry of simplicial lattices is in fact crucial to the numerical success of ref. [4]. From the previous section one sees that the faces c_{ij} (and $c_{ij}{}^\sigma$) will be especially important.

In each dual cell one can locally fix to radial gauge, $(x - x_i) \cdot A^{(i)} = 0$. The link ℓ_{ij} from x_i to x_j is a radial path in both c_i and c_j, so parallel transport from i to j along ℓ_{ij} is (see fig. 1):

$$\mathrm{P}\exp\left[\int_x \mathrm{d}x \cdot A^{(i)}(x)\right] v_{ij}(x_{ij}) \mathrm{P}\exp\left[\int_x \mathrm{d}x \cdot A^{(j)}(x)\right] = v_{ij}(x_{ij}) = U_{ij}, \quad (3.1)$$

where U_{ij} is the gauge group matrix associated with ℓ_{ij}, and the second equality follows from the usual interpretation of U_{ij}. In the local radial gauge, however, U_{ij} also has the interpretation as the transition function at x_{ij}, the midpoint of ℓ_{ij}. The reconstruction of a bundle now involves defining transition functions at *all* points on the faces of the dual cells.

To effect this extension Phillips and Stone order the vertices of each simplex, $\sigma = \langle 0, 1, 2, \ldots, d \rangle$, restrict attention to the c_i^σ, and introduce appropriate coordinates for the $d-1$ dimensional faces $c_{ij}{}^\sigma$. If i and j are adjacent according to the ordering, then v_{ij} remains constant for all $x \in c_{ij}{}^\sigma$. If i and j are not adjacent, but rather separated by $1 \leqslant n \leqslant d-1$ vertices, then the interpolation of v_{ij} depends on the n coordinates corresponding to the interposed vertices. Consider, for example, two dimensions, where a simplex is a triangle, $\sigma = \langle 0, 1, 2 \rangle$, depicted in fig. 2. At all

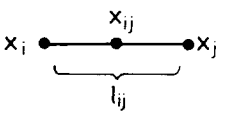

Fig. 1. Viewed from each endpoint, x_i and x_j, the link ℓ_{ij} is a radial path.

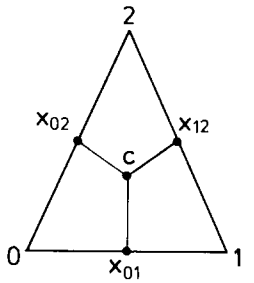

Fig. 2. The 2-simplex $\sigma = \langle 0,1,2 \rangle$. The bundle is determined first on the midpoints x_{ij}, then on the segments towards the center C, and finally in the interior.

three midpoints the condition (3.1) determines the transition functions v_{01}, v_{12}, and v_{02}. On the line segment $\overline{x_{01}\mathrm{C}}(\overline{x_{12}\mathrm{C}})$ the transition function $v_{01}(v_{12})$ is constant. At the center of the triangle C,

$$v_{02}(\mathrm{C}) = v_{01}(\mathrm{C})\, v_{12}(\mathrm{C}), \tag{3.2}$$

by the cocycle condition. The smoothest interpolation along $\overline{x_{02}\mathrm{C}}$ is the geodesic from U_{02} to $U_{01}U_{12}$. Hence,

$$v_{02}(z_1) = U_{02}(U_{20}U_{01}U_{12})^{z_1}, \tag{3.3}$$

where $0 \leqslant z_1 \leqslant 1$ is the coordinate parametrizing $\mathrm{c}_{02}{}^{\sigma}$. In higher dimensions the construction continues according to the following principles: eq. (3.1), the cocycle condition (3.2), induction on the dimension, and geodesic interpolation à la (3.3). Since the construction becomes rather intricate, we refer the reader to ref. [4] for details.

Phillips and Stone [4] also provide a section. In σ the section $g_i{}^{\sigma}$ has zero winding number on all $\partial \mathrm{c}_i{}^{\sigma}$ *except* $\partial \mathrm{c}_0{}^{\sigma}$, which has the topology of S^3. Although we do not wish to give detailed formulae or a detailed description of the section, we would like to give an indication of its geometric structure, and, more importantly, of the computation necessary for evaluating the winding numbers. $\mathrm{c}_0{}^{\sigma}$ is geometrically a hypercube; the 16 corners compose $\{ p \,|\, p = p_0 + \Sigma a_i p_i,\ a_i \in \{0, \frac{1}{2}\}\}$, i.e. the site 0, the midpoints of the links radiating from 0, and certain points in the interior of σ. The section maps each of the corners to a parallel transporter inside the simplex σ, i.e. to a product of link matrices. The section on $\partial \mathrm{c}_0{}^{\sigma}$ naturally splits $\partial \mathrm{c}_0{}^{\sigma}$ into its eight faces. Six of these faces are split by the interpolating functions into four tetrahedra and a quadrilateral-based pyramid. The other two are split into two triangular prisms. More precisely, a tetrahedron, for example, of space-time is mapped to a spherical tetrahedron in $\mathrm{S}^3 = \mathrm{SU}(2)$, etc.

To decide if the probe is in a tetrahedron or a prism, one must only compute determinants of 4×4 matrices whose columns are given by vertices of the spherical tetrahedron/prism (written as a vector in $\mathbb{R}^4$). The sign of these determinants indicates the position of the probe relative to the sides of the tetrahedron or prism.

The pyramid is harder to analyze because of the shape of the base. The pyramid is part of a cone in S^3 with four triangular faces. The position of the probe relative to these faces is again given by 4×4 determinants. If the probe is *inside* the cone, then the number of times it falls inside the pyramid is 0, 1, or 2 and equal to the number of real, positive roots of a quadratic equation describing the base.

In conclusion, Phillips' and Stone's interpolation [4] reduces the calculation of the SU(2) topological charge to the computation of 4×4 determinants and of the roots of quadratic equations. The importance of the fact that $S^3 = SU(2)$ should not be underestimated. Their interpolation also defines transition functions for SU(3). However, as far as we are aware, no one has sufficiently mastered the analytic geometry of SU(3) to reduce computation of Q to fast arithmetic operations. Instead, the functions defining the section must be interpolated explicitly to discover the "singularities" or "vortices" – points where the winding of the SU(2) subgroups is concentrated.

4. Implementation on a hypercubic lattice

In order to exploit this algorithm on a hypercubic configuration one must slice a hypercube into simplices. The minimal procedure [15] is as follows: number the vertices of a hypercube from 0 to 15 as in fig. 3; if one writes the numbers in binary, the bits correspond to the coordinates of the vertices, taking 0 as the origin. Consider the vertices with an even number of unit bits $\{0, 3, 5, 6, 9, 10, 12, 15\}$. Draw plaquette diagonals between pairs chosen from this set that differ by exactly two bits, e.g. from $3_{10} = 0011_2$ to $9_{10} = 1001_2$ – the second and fourth bits differ. There

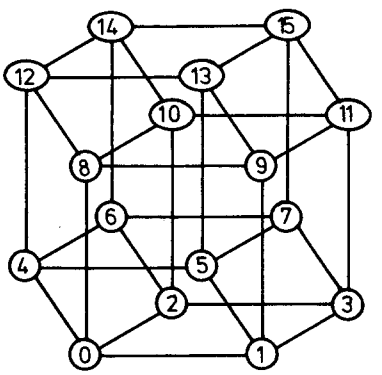

Fig. 3. Numbering of the vertices in a generic hypercube.

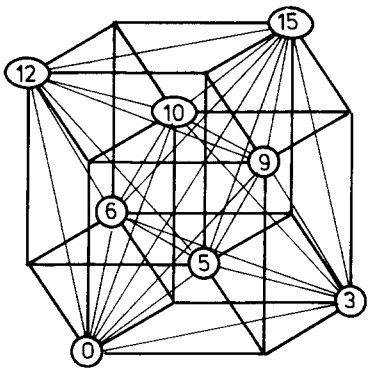

Fig. 4. The new links: 24 plaquette diagonals and one-body diagonal.

are 24 such diagonals. Finally, draw a new link from 0 to 15 – a body diagonal. The sliced hypercube is sketched in fig. 4; there are sixteen simplices:

$$[0,1,3,5,9],[0,2,3,6,10],[0,4,5,6,12],[0,8,9,10,12],$$

$$[3,5,6,7,15],[3,9,10,11,15],[5,9,12,13,15],[6,10,12,14,15],$$

$$[0,3,5,9,15],[0,3,6,10,15],[0,5,6,12,15],[0,9,10,12,15],$$

$$[0,3,5,6,15],[0,3,9,10,15],[0,5,9,12,15],[0,6,10,12,15]. \qquad (4.1)$$

With the help of fig. 5, it is not difficult to visualize how these sixteen simplices fill a hypercube.

To triangulate a hypercubic lattice into a simplicial complex one must take care to treat the 3-cubes at the intersections compatibly. For example, having sliced a

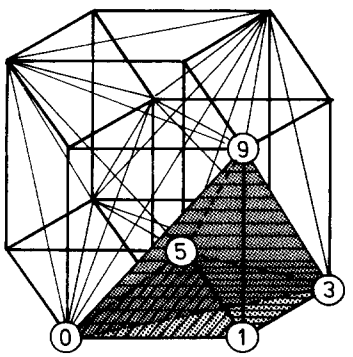

Fig. 5. The simplex [0,1,3,5,9] illustrates how the hypercube is triangulated.

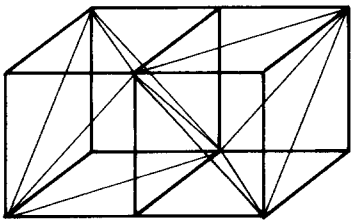

Fig. 6. Even in three dimensions the minimal triangulation requires reflection of the generic cube.

given hypercube, one cannot translate it to one of its neighbors; instead one must reflect about the common 3-cube. The need for reflection is not peculiar to four dimensions; it is necessary already for $d = 3$, as shown in fig 6. Continued reflections will build up a 2^4 block, and then translation of the 2^4 block will complete the triangulation. Note that this provides the mild requirement that we use lattices whose sides are an even multiple of the lattice spacing long.

The next step is to define parallel transporters for the new links. For the 24 plaquette diagonals we choose the element of SU(2) so that parallel transport around the two triangles is "half" that around the plaquette: i.e.

$$U_{03} = U_{02}U_{23}(U_{32}U_{20}U_{01}U_{13})^{1/2}. \tag{4.2}$$

For the body diagonal there are now three "grand plaquettes" across which we can interpolate: $\langle 0,3,15,12,0\rangle$, $\langle 0,5,15,10,0\rangle$, and $\langle 0,6,15,9,0\rangle$. We want to pick the body diagonal that yields, on the whole, the configuration with the smallest parallel transport around closed loops. We should therefore interpolate, as in eq. (3.5), using the path with the *largest* parallel transport, which makes the field on the associated grand plaquette as smooth as possible.

Lasher, Phillips, and Stone [3] have also implemented the simplicial algorithm on a hypercubical lattice. However, they decompose a hypercube into 24 simplices, rather than our 16. Consequently, our program was originally $1\frac{1}{2}$ times faster. The algorithm (see above) dictates that the program spends most of the time evaluating 4×4 determinants. During testing and debugging the program we noticed that it is important to evaluate the determinants (and the roots of the quadratic equation) in double precision (64-bit) arithmetic, especially for smooth "instanton" configurations obtained by cooling. Using single precision (32-bit) arithmetic the program frequently concluded that the probe was on the wrong side of the faces of the spherical solid figures. Double precision costs more time, but we realized how to recoup this loss. Ref. [4] mandates the complete list of determinants; most of them involve the unit vector $\boldsymbol{I} = (1,0,0,0)$, which effectively reduces them to 3×3 determinants. Moreover, most of the determinants also involve the probe $\boldsymbol{Y}$, and the choice $\boldsymbol{Y} = (0,-1,0,0)$, for example, effectively reduces $4 \times 4(3 \times 3)$ to $3 \times 3(2 \times 2)$

determinants. (Recall that the charge is independent of the probe.) Making these reductions explicit in the program yields a tremendous saving in time.

Table 1 compares the IBM-3081 CPU time for 6^4 lattices for four algorithms: (i) integration [1] of the transition function expression (2.11) using Lüscher's bundle [10]; (ii) the method [13] mentioned in sect. 2 using the section for Lüscher's bundle [14]; (iii) Lasher et al. [3]; and (iv) our present program. The first two methods will become faster for smoother configurations (higher β) and the table is based on $\beta = 2.2$. We should also add that method (ii) [13] was not fully optimized, because it was abandoned in favor of the fastest option.

5. Numerical results

In this section we present our numerical results. Using the standard heat bath updating algorithm, we generated sequences of configurations distributed according to the Boltzmann distribution of the Wilson plaquette action

$$S = \tfrac{1}{2}\beta \sum_{\mathrm{p}} \mathrm{tr}\{\mathbf{1} - U(\partial \mathrm{p})\} \tag{5.1}$$

for several values of the SU(2) coupling β. In eq. (5.1), $U(\partial \mathrm{p})$ denotes the parallel transporter around the plaquette p. All of our runs began with cold starts and > 1000 sweeps for thermalization. For 6^4 lattices the program ran so fast that we discarded 50 configurations between those for which the charge was determined. For larger lattices we kept a closer eye on previous experience, which indicated decorrelation times of ≈ 10 sweeps [16] for our range of β, and thus determined the charge after every 15 update sweeps. We occasionally observe several tens of successive configurations with the same charge, yet any quantitative measure of the correlations would indicate that separations of 15 sweeps suffice. (Note, though, that the statistical analysis is affected by the fact that the charge is always an integer.)

Table 2 contains our numerical results for $a^4\chi_t$ (a is the lattice spacing) for 6^4, 8^4, and 10^4 lattices at $\beta = 2.2$–2.6. This table also indicates the number of configurations N_{tot} in each Monte Carlo sample. We estimated the error by dividing the samples into bins of N_{bin} successive configurations and computing the susceptibility for the individual bins. For the runs with moderate statistics we took

TABLE 1
Comparison of CPU time for various algorithms on a 6^4 lattice

method	1	2	3	4
reference	[1]	[13]	[3]	this work
IBM-3081	40 min	3 min	3 min	30 sec

TABLE 2
Compilation of $a^4\chi_t$ from this work

β	V	$a^4\chi_t$	N_{tot}
2.2	6^4	$(7.45 \pm 1.17) \times 10^{-3}$	450
2.3	6^4	$(2.85 \pm 0.31) \times 10^{-3}$	250
2.3	10^4	$(3.06 \pm 0.11) \times 10^{-3}$	800
2.4	6^4	$(7.56 \pm 1.08) \times 10^{-4}$	200
2.4	8^4	$(10.12 \pm 0.61) \times 10^{-4}$	1600
2.4	10^4	$(11.14 \pm 0.21) \times 10^{-4}$	4000
2.5	6^4	$(2.78 \pm 0.46) \times 10^{-4}$	200
2.5	10^4	$(3.26 \pm 0.20) \times 10^{-4}$	800
2.6	10^4	$(1.08 \pm 0.15) \times 10^{-4}$	400

$N_{bin} = 50$ or 100, depending on N_{tot}. At $\beta = 2.4$ we have high statistics on 8^4 lattices and very high statistics on 10^4 lattices. We could therefore look at a wide range of binsizes from $N_{bin} = 200$ to 800; in this range the error estimates do not change, so we are confident that we have realistically determined the statistical error inherent to the Monte Carlo technique.

The high statistics at $\beta = 2.4$ allow us to address finite volume effects. From table 2 one sees that $a^4\chi_t$ increases as V increases from 6^4 to 8^4 to 10^4 at $\beta = 2.4$. From 6^4 to 8^4 the susceptibility changes by 30%, whereas from 8^4 to 10^4 the change is only 10%. Such a trend is in qualitative agreement with the conventional wisdom [17] for the limit $V \to \infty$, β fixed, and provides us with confidence that the finite volume effects are under control, and that they are quite likely small for the $V = 10^4$, $\beta = 2.4$ simulation. Indeed, other applications [5] motivated this long run: it seemed to offer the best compromise between infrared and ultraviolet cutoff

TABLE 3
Charge Q and the number $N_Q^+(N_Q^-)$ of configurations with charge $+Q(-Q)$

Q	N_Q^-	N_Q^+
0	322 ± 29	
1	279 ± 17	274 ± 17
2	200 ± 11	176 ± 4
3	95 ± 12	119 ± 11
4	45 ± 4	57 ± 6
5	10 ± 7	10 ± 5
6	4 ± 2	7 ± 3
7	1	0
8	0	1

Simulation on a 8^4 lattice at $\beta = 2.4$. Of course, $Q = 0$ has only one entry.

TABLE 4
Same as table 3, but for a 10^4 lattice

W	N_Q^-	N_Q^+
0	451 ± 15	
1	520 ± 15	465 ± 20
2	413 ± 23	382 ± 18
3	329 ± 20	305 ± 12
4	221 ± 17	207 ± 12
5	141 ± 12	161 ± 13
6	85 ± 8	108 ± 8
7	57 ± 8	57 ± 4
8	26 ± 7	29 ± 7
9	10 ± 3	11 ± 4
10	6 ± 2	8 ± 3
11	3 ± 2	1
12	1	1
13	1	0
14	1	0

errors, given our computer resources and the status of the susceptibility computations.

For the connoisseur tables 3 and 4 and figs. 7 and 8 show the distributions for the high statistics simulations on the 8^4 and 10^4 lattices, respectively. From these data one can verify that $\langle Q \rangle = 0.054 \pm 0.050$ for 8^4 and $\langle Q \rangle = -0.001 \pm 0.004$ for 10^4. The peak at $Q = -1$ in the 10^4 histogram is apparently just a statistical fluctuation, coming from the third bin of 800 configurations; amusingly enough, the $\langle Q \rangle$ for that bin is actually positive.

Since we are now able to compute the topological susceptibility very quickly, χ_t becomes a viable candidate observable for studying scaling and the approach to the continuum limit in lattice gauge theories. The computation is very clean: no fitting is required, in contrast to the string tension, mass gaps, or phase transition temperatures. The main drawback is that the relation to easily (experimentally) measured quantities is rather indirect, coming through approximate expressions like eq. (1.4). Nevertheless, taken in conjunction with the recent precise calculations of the SU(2) quark potential (string tension) [18], further work on the topological susceptibility could demonstrate if there is a window in β with universal, if not asymptotic two-loop, scaling. Note that the error on χ_t at $\beta = 2.4$ on the 10^4 lattice is already comparable to that on K in the high statistics computation in ref. [18].

In anticipation of such future studies we discuss asymptotic scaling and the topological susceptibility. In fig. 9 we plot $a^4\chi_t$ as a function of β. The curve represents the two-loop renormalization group formula for the lattice spacing a:

$$a = \Lambda_L^{-1}\left(\tfrac{6}{11}\pi^2\beta\right)^{51/121}\exp\left(-\tfrac{3}{11}\pi^2\beta\right), \tag{5.2}$$

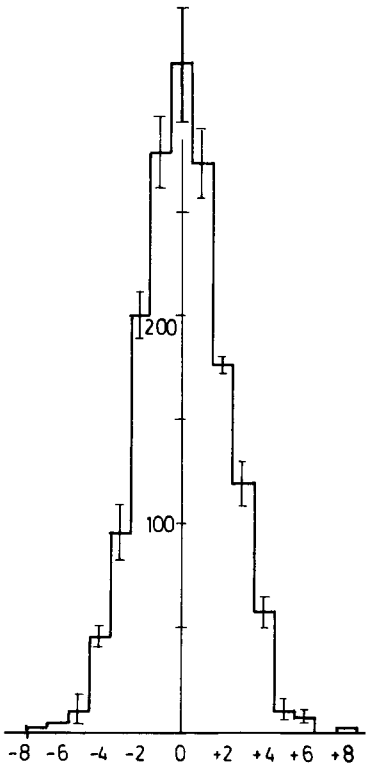

Fig. 7. Charge distribution on a 8^4 lattice at $\beta = 2.4$.

raised to the fourth power and normalized to the high statistics simulation at $V = 10^4$, $\beta = 2.4$. Here Λ_L is the lattice scale parameter. Table 5 gives values of $10^6 \chi_t / \Lambda_L^4$ assuming (5.2), as well as those of Fox et al. [1] (using Lüscher's bundle [10]), Arian and Woit [2] (using Woit's latest algorithm [19]), and Lasher et al. [3] (using Phillips' and Stone's bundle [4], but with 24 simplices rather than 16, cf. sect. 4). The 6^4 lattice computations of the susceptibility show some mutual agreement, especially for $\beta \geqslant 2.4$. Some also provide evidence of two-loop scaling for $\beta \geqslant 2.3$. However, the errors are so large and the lattices are so small that the agreement and the scaling are misleading, especially at the larger values of β, where the physical volume is miniscule. The simulations on 10^4 lattices support such skepticism: the asymptotic scaling window is broken. Moreover, the topological susceptibility shows the *same* scaling violations as the string tension K. In fact, using the results of ref. [20] we find that the ratio

$$a^4 \chi_t / a^4 K^2 \tag{5.3}$$

is constant over the whole range of β values listed in table 5. We should mention,

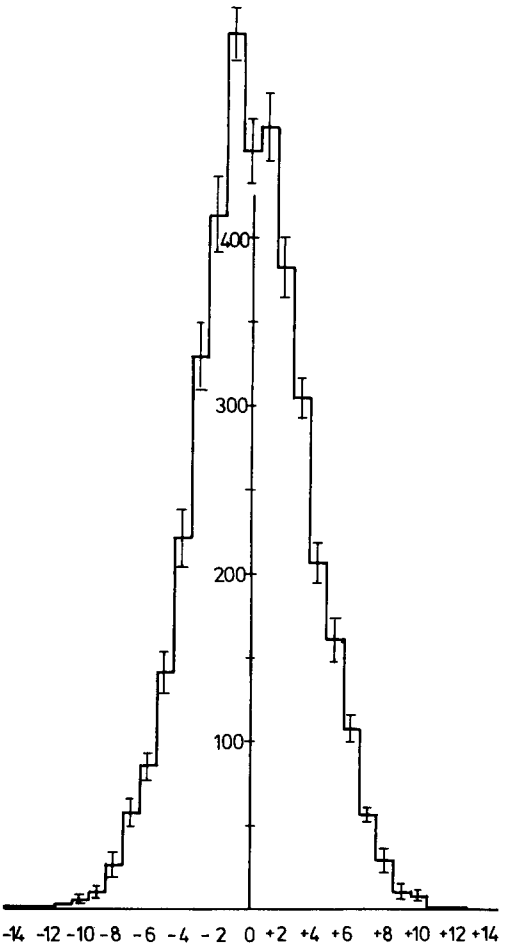

Fig. 8. Same as fig. 7, but for a 10^4 lattice.

though, that the finite volume corrections at $\beta \geqslant 2.5$ might alter the values of $a^4\chi_t$ slightly.

With some reservation we offer, finally, the topological susceptibility in physical units. To do so, we need $\Lambda_L = 6.6$ MeV, based on the string tension calculation of ref. [20] at $\beta = 2.4$. Using the $V = 10^4$, $\beta = 2.4$ simulation we find

$$\chi_t = (262 \pm 1 \text{ MeV})^4. \tag{5.4}$$

Averaging the 10^4 column of table 5 does not change χ_t significantly, because the error at $\beta = 2.4$ is so small that it dominates the (weighted) average. The result (5.4) is the same magnitude as the large N_c prediction (1.4), but not in quantitative

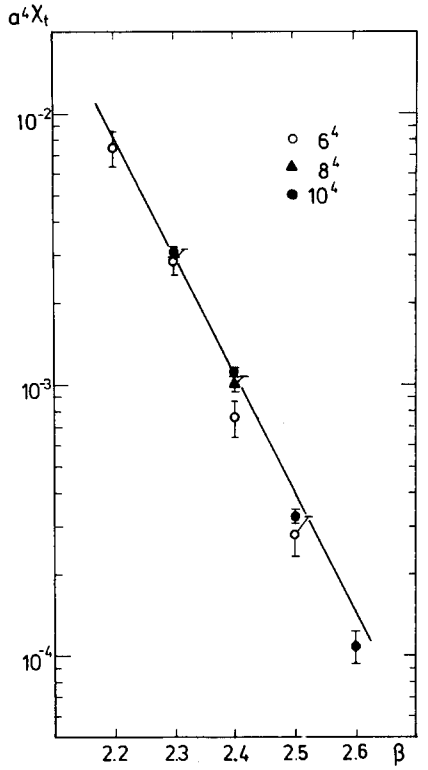

Fig. 9. The topological susceptibility $a^4\chi_t$ from this work.

TABLE 5
Compilation of $10^6\chi_t/\Lambda_L^{-4}$ from this work and other recent publications [1–3]

β	this work, 10^4	this work, 6^4	ref. [1], 6^4	ref. [2], 6^4	ref. [3], 6^4
2.2		2.23 ± 0.35	1.90 ± 0.33	2.12 ± 0.60	1.29 ± 0.12
2.3	2.51 ± 0.09	2.29 ± 0.24	2.76 ± 0.30	2.11 ± 0.53	1.77 ± 0.16
2.4	2.48 ± 0.05	1.70 ± 0.25	2.43 ± 0.26	1.38 ± 0.40	1.91 ± 0.21
2.5	1.99 ± 0.12	1.69 ± 0.30	2.51 ± 0.29	1.29 ± 0.39	1.69 ± 0.28
2.6	1.79 ± 0.12				

agreement. However, considering the limitations of the large N_c expansion, the assumption of universality, and systematic effects of the numerical simulation, the agreement is quite satisfactory.

Alternatively, one can assume that eq. (1.4) holds. Then our result (5.4) yields a prediction of the η' mass:

$$m_{\eta'} = 1854 \text{ MeV} \tag{5.5}$$

compared to the experimental value 958 MeV.

6. Universality

There are various ways to assign a smooth bundle to a lattice gauge field. The interpolations of Lüscher [10] and of Phillips and Stone [4] are only two examples. While deep in the continuum limit all of the interpolated fields have the same topological charge, this is not guaranteed at the values of β discussed in the previous section. Indeed, we have compared Lüscher's bundle with Phillips' and Stone's bundle on a configuration by configuration basis. On a 6^4 lattice at $\beta = 2.5$ the two definitions agree in only 66% of the cases, while in 28% (6%) of the cases they disagree by 1 (2) units. There is a tendency, though, that the agreement improves as β is increased. Moreover, the topological susceptibility appears to be the same for both bundles.

The origin of this discrepancy lies in the fluctuations of the gauge field at the scale of a lattice spacing. These have no genuine topological meaning, and, unlike smoothly varying fields, contribute differently in different interpolation schemes. Consequently, one cannot assign a unique topological charge to lattice gauge configurations with large fluctuations on the shortest scales. In the following we shall argue, however, that the contribution of these short distance fluctuations to the topological *susceptibility* is exponentially suppressed compared to the contribution of the smoother fields.

The contribution of the small scale fluctuations can be calculated [21] by finding the minimum action $S_{\min}$ of a configuration with $|Q| = 1$. At most $S_{\min}$ is the action of a one (anti-)instanton configuration, but at least that of an exceptional configuration [10] bounding the $|Q| = 1$ configurations. One can determine the value of $S_{\min}$ numerically by monitoring Q and S during "cooling" runs. We have done this for configurations from the equilibrium ensemble, and for instanton configurations. Both runs indicate that

$$S_{\min} \geq 12\beta . \tag{6.1}$$

We find, among others, minimal action configurations where the six plaquettes surrounding a certain link have $\mathrm{tr}\{U(\partial \mathrm{p})\} \approx -2$ and the rest have $\mathrm{tr}\{U(\partial \mathrm{p})\} \approx +2$.

Assume a dilute gas of the minimum action configuration, which is justified because the correlation between the small scale fluctuations is an exponential characterized by the 0^- glueball mass. Then the contribution to the susceptibility is

$$\chi_t^{\text{small scale}} \sim \beta^{-1} \exp(-12\beta) . \tag{6.2}$$

Since the renormalization group predicts (cf. eq. (5.2))

$$\chi_t \sim \left(\tfrac{6}{11}\pi^2\beta\right)^{204/121} \exp\left(-\tfrac{12}{11}\pi^2\beta\right), \tag{6.3}$$

and since $12 > 12\pi^2/11 = 10.77$, the fluctuations on a scale well below the correla-

tion length will not effect the topological susceptibility. We therefore expect that χ_t obeys the same scaling law as other physical observables, and that its value is universally defined even for ensembles containing configurations for which the charge is not unique.

7. Conclusions

These calculations show that it is now possible to perform a solid computation of the topological susceptibility using numerical simulations. The fast algorithm [4] allows us to achieve high statistics on large lattices in a reasonable amount of computer time. For example, the run with a Monte Carlo sample of 4000 configurations took around 500 hours on the University of Hamburg Siemens-Fujitsu 7882, which ran about as fast as the IBM-3081. The charge program is readily vectorizable. The string tension, glueball masses, and phase transition temperatures require ansätze for fits, but χ_t does not: we compute it directly. The topological susceptibility is therefore competitive with other physical quantities as a probe of the SU(2) gauge theory.

One would like to extend these calculations to the physically more interesting gauge group SU(3). The interpolation of ref. [4] exists for SU(3), but the algorithm for the charge computation does not. Barring a breakthrough in that direction, the method of ref. [13] seems most promising, perhaps in conjunction with the reduction of SU(3) to SU(2) [22, 11]. Eventually, we hope to test the intriguing ideas [23] linking topology to confinement.

We are grateful to the computing centers of the Universities of Hamburg, Berlin, and Hannover and of NORDITA for time on their computers; in particular we thank B. Nilsson for assistance on the new VAX-8600 at NORDITA. It is a pleasure to acknowledge pleasant conversations with F. Gutbrod, M. Lüscher, and A. Phillips on various aspects of this work. We thank C. Schleiermacher for help with the computation, especially the data analysis. Two of us (M.L.L. and U.J.W.) would also like to thank R. Peccei for frequent hospitality at DESY.

References

[1] I.A. Fox, J.P. Gilchrist, M.L. Laursen, and G. Schierholz, Phys. Rev. Lett. 54 (1985) 749
[2] Y. Arian and P. Woit, Nucl. Phys. B268 (1986) 521
[3] G. Lasher, A. Phillips, and D. Stone, *in* Quark confinement and liberation: Numerical results and theory, eds. F. Klinkhammer and M.B. Halpern (World Scientific, Singapore, 1985)
[4] A. Phillips and D. Stone, Commun. Math. Phys. 103 (1986) 599
[5] A.S. Kronfeld, M.L. Laursen, G. Schierholz, C. Schleiermacher, and U.-J. Wiese, in preparation
[6] D. Gross, R. Pisarski, and L. Yaffe, Rev. Mod. Phys. 53 (1981) 43
[7] P. van Baal, Commun. Math. Phys. 85 (1982) 529
[8] E. Witten, Nucl. Phys. B156 (1979) 269;
G. Veneziano, Nucl. Phys. B159 (1979) 213

[9] P. di Vecchia, K. Fabricius, G.C. Rossi, and G. Veneziano, Nucl. Phys. B192 (1981) 392;
K. Ishikawa, G. Schierholz, H. Schneider, and M. Teper, Phys. Lett. 128B (1983) 309
[10] M. Lüscher, Commun. Math. Phys. 85 (1982) 29
[11] M. Göckeler, M.L. Laursen, G. Schierholz, and U.-J. Wiese, Commun. Math. Phys. 107 (1986) 467
[12] M.L. Laursen, G. Schierholz, and U.-J. Wiese, Commun. Math. Phys. 103 (1986) 693
[13] M. Göckeler, A.S. Kronfeld, M.L. Laursen, G. Schierholz, and U.-J. Wiese, Nucl. Phys. B292 (1987) 349
[14] U.-J. Wiese, Universität Hannover thesis (1986)
[15] M.L. Laursen, G. Schierholz, and U.-J. Wiese, unpublished;
M. Lüscher, unpublished.
[16] K. Ishikawa, G. Schierholz, and M. Teper, Z. Phys. C19 (1983) 327
[17] M. Lüscher, Nucl. Phys. B205 (1982) 483
[18] F. Gutbrod, Z. Phys. C30 (1986) 585
[19] P. Woit, Nucl. Phys. B262 (1986) 284
[20] F. Gutbrod and I. Montvay, Phys. Lett. 136B (1984) 411
[21] M. Lüscher, Nucl. Phys. B200 (1982), 61
[22] G. Parisi and F. Rapuano, Phys. Lett. 152B (1985) 218
[23] See, for example, G. 't Hooft, Acta Phys. Austr., Suppl. XXII (1980) 531